

# Topological Flexural Modes in Polarized Bilayer Lattices

Mohammad Charara,<sup>1</sup> Kai Sun,<sup>2</sup> Xiaoming Mao,<sup>2</sup> and Stefano Gonella<sup>1,\*</sup>

<sup>1</sup>*Department of Civil, Environmental, and Geo- Engineering,  
University of Minnesota, Minneapolis, MN 55455, USA*

<sup>2</sup>*Department of Physics, University of Michigan, Ann Arbor, Michigan 48109, USA*

Topological lattices have recently generated a great deal of interest based on the unique mechanical properties rooted in their topological polarization, including the ability to support localized modes at certain floppy edges. The study of these systems has been predominantly restricted to the realm of in-plane mechanics, to which many topological effects are germane. In this study, we stretch this paradigm by exploring the possibility to export certain topological attributes to the flexural wave behavior of thin lattice sheets. To couple the topological modes to the out-of-plane response, we assemble a bilayer lattice by stacking a thick topological kagome layer onto a thin twisted kagome lattice. The band diagram reveals the existence of modes whose out-of-plane character is controlled by the edge modes of the topological layer, a behavior elucidated via simulations and confirmed via laser vibrometer experiments on a bilayer prototype specimen. These results open a new direction for topological mechanics whereby flexural waves are controlled by the in-plane topology, leading to potential applications for flexural wave devices with engineered polarized response.

Lattice materials are mechanical systems featuring a unit cell repeated periodically in space. Maxwell lattices are a special subset of lattices characterized by having an equal number of degrees of freedom and constraints [1], thus being on the verge of mechanical instability [2–5]. A prototypical example in two dimensions is the kagome lattice, whose unit cell is composed of two triangles hinged at a vertex, which has garnered considerable attention for its mechanical properties [6–9], tunable wave propagation characteristics [10–14], and for its potential for reconfigurability and property tuning [15, 16].

Some of the most interesting phenomena arise at the boundaries of finite domains [17–19]. Certain edge properties are conceptually analogous to those observed in electrical or quantum systems, such as topological insulators [20–23]. Recently, a subclass of Maxwell lattices has been shown to exhibit topological behavior [2, 24, 25], whereby they possess the ability to localize deformation on one edge of the lattice (denoted as the floppy edge) in the form of zero-frequency floppy modes, while the opposite edge is rigid. Although the topological properties manifest at the edges, they are, in fact, intrinsic to the bulk, a property known as bulk-edge correspondence. Further, the topological behavior has been shown to be tunable via a cell reconfiguration, obtained by subjecting the lattice to global zero energy soft strains, which can cause phase transitions between polarized and non-polarized states [26].

Analogous phenomena have also been realized in structural lattices, an exercise that requires relaxing the perfect hinges to finite-thickness ligaments with the ability to support in-plane bending [27, 28]. As a result, the floppy modes have been shown to rise to finite frequencies, but the signature of polarization persists in the abil-

ity to localize deformation on the lattice soft edge.

Thus far, investigations of the topological behavior of 2D Maxwell lattices have been predominantly restricted to their native in-plane mechanics, without exploring its broader implications for their out-of-plane response. While extensions of topological mechanics to 3D domains have been proposed [29–31], our focus here is on the out-of-plane response of systems whose periodicity remains strictly two-dimensional. In this letter, we attempt to address this gap by answering the following questions. Are the topological modes of structural Maxwell lattices exportable to the out-of-plane realm? If so, with what degree of dilution? The answer to these questions will be obtained by performing Bloch analysis and full-scale simulations involving fully 3D lattice models, and corroborated by laser vibrometry experiments.

To promote coupling between in-plane and out-of-plane mechanics in a thin structure, we need to establish some degree of stiffness non-uniformity through its thickness - obtained by modulating either the material properties or the geometric cross-sectional characteristics - and/or to impose a loading stimulus with some eccentricity. In lattice metamaterials, a natural avenue to modulate the equivalent stiffness is by tuning the unit cell geometry. This modulation can be either continuous through the thickness (as in a functionally graded structure), or piece-wise uniform (as in a multilayer composite). Consider, for instance, a bilayer beam obtained by stacking a soft layer on a thinner layer that is stiffer in-plane but retains high flexural compliance due to its thinness. Intuitive structural mechanics considerations suggest that an in-plane state of strain established in the soft layer would result in coupling to an out-of-plane (flexural) deformation experienced globally by the bilayer (1a). These bending kinematics would necessarily emerge as a result of the difference in the ability of the two layers to accommodate in-plane deformation, along with the

\* sgonella@umn.edu

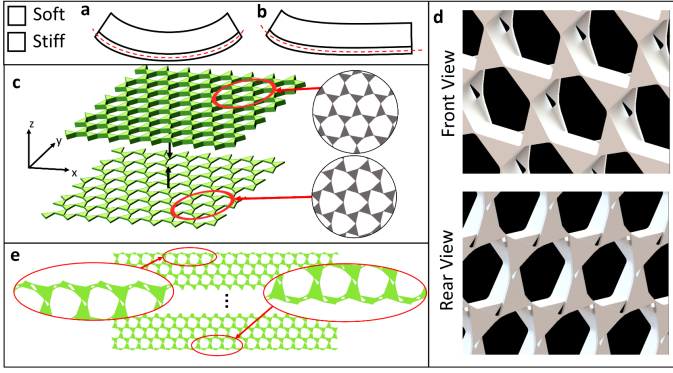


FIG. 1. (a) Schematic of coupling-induced bending in a bilayer structure due to strain in the soft layer; (b) localized bending due to excess of softness on one edge of the soft layer; (c) bilayer lattice assembly strategy; (d) close-up details of the front and rear face of the lattice; (e) details of the trimmed top and bottom edges.

compatibility requirements at their interface, and of the eccentricity of the applied stimulus. This concept is commonly invoked in the design of bimorphs working as flexural actuators [32], or in the excitation of flexural waves in thin plates by means of piezoelectric patches subjected to voltage stimuli [33].

For a conventional bilayer structure in which the mismatch of in-plane deformability is established over the entire domain, such in-plane to out-of-plane coupling is available across the entire domain. Suppose instead that the state of strain induced in a layer is localized at one boundary, as in the floppy modes of topologically polarized lattices. By the same logic, we can conjecture that the resulting coupling will also display an analogous degree of localization, and the bilayer will display the ability to localize bending deformation asymmetrically at the edges (Fig. 1b). The remainder of this Letter is devoted to demonstrate this connection and quantify the signature of the polarization effects available for bending modes.

To explore this idea, we propose a bilayer structure consisting of a topological kagome lattice stacked on a non-polarized twisted kagome lattice (Fig. 1c). The roles of the two layers are distinct and complementary. The topological layer provides the in-plane polarization required to trigger the desired topological edge behavior. The twisted kagome merely provides some impedance against the deformation mechanisms germane to the floppy mode of the topological layer, thus promoting out-of-plane coupling by establishing the required through-the-thickness eccentricity. In light of these considerations, we make the twisted kagome layer as thin as practically realizable to maximize its flexural compliance while maintaining its nominal in-plane stiffness. This also ensures that the in-plane mechanics of the bilayer are predominantly controlled by the topological layer. Based

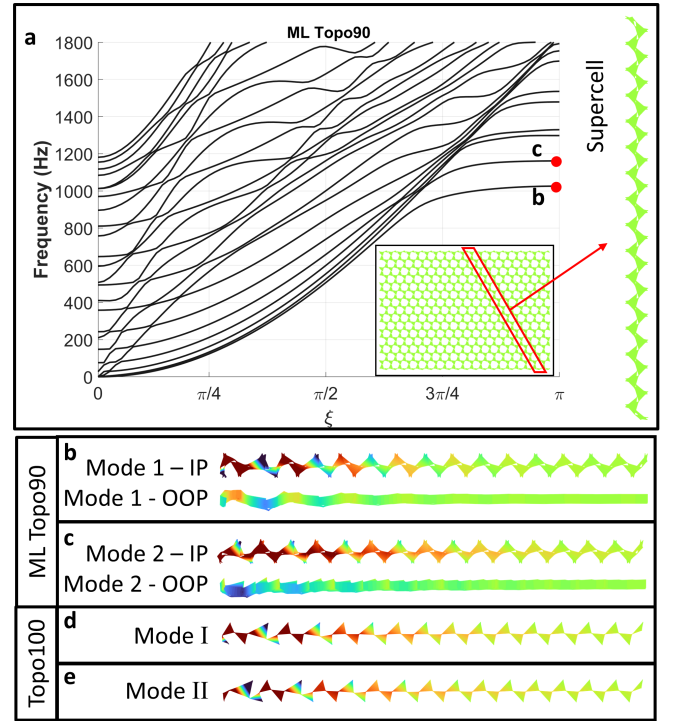


FIG. 2. Band Diagram of 16-cell supercell for ML Topo90 with mode shapes for the first two modes at  $\pi$  (b,c); edge mode mode shapes at  $\pi$  for Topo100 (d,e) shown for reference

on these considerations, in our design, 90% of the total thickness is occupied by the topological layer and 10% by the twisted kagome layer. Henceforth, we refer to this bilayer configuration as ML Topo90. The triangles in the twisted kagome feature 2.35 cm sides, 0.12 cm thick hinges, and a twist angle of  $16.4^\circ$ . The topological layer has two scalene triangles with side lengths 2.82 cm, 2.45 cm, and 2.18 cm, and 0.12 cm thick hinges. The total thickness of ML Topo90 is 1.65 cm. High resolution isometric close-up renderings of the front and rear face are shown in Fig 1d. In anticipation of a comparison carried out later, it is helpful to define a reference lattice consisting solely of the topological layer of ML Topo90 taken in isolation, which we refer to as Topo100. Throughout our analysis, we assume all lattices are made from acrylonitrile butadiene styrene (ABS) plastic ( $E = 2.14$  GPa,  $\nu = 0.35$ ), although these results are scalable to other materials. Note that we deliberately amend the lattice edges by trimming, as much as possible, the protruding portion of the edge cells (Fig. 1e) to minimize any edge-localized trivial effects that may disrupt our observation of the topological edge effects we are actually after, an operation that is fair to perform by invoking the notion of topological edge protection (see SM).

Fig. 2a shows the band diagram (BD) for an ML Topo90 16-cell supercell, modeled using 3D elasticity. The coexistence of in-plane and out-of-plane modes results in a richer, denser, and highly hybridized band spec-

trum compared to the prototypical case of a topological lattice deforming in-plane, such as the one studied in Ma et al. [27]. This additional modal complexity poses a challenge for the proper identification of any topologically polarized modes. Since in the 2D model of a single layer the modal density at low frequencies is low, the topological edge modes live in the frequency interval in which the only other available modes are the in-plane acoustic modes, which can be easily discriminated from the topological ones due to the evident wavelength mismatch. In a 3D model (of a bilayer), the edge modes are forced to co-exist with a plethora of flexural modes. Therefore, their identification cannot rely solely on the spectral characteristics of the branches, but must involve a morphological inspection of the associated mode shapes. We focus our attention on the first two ML Topo90 modes for  $\xi \rightarrow \pi$ , where the topological edge modes are most localized in 2D elasticity. Their mode shapes at  $\xi = \pi$  are shown in Fig 2b, and 2c for mode 1 and 2, respectively, with in-plane deformation shown in the top-down view (color proportional to in-plane displacement in the  $y$  direction) and out-of-plane deformation shown in the side view (color proportional to out-of-plane displacement). For comparison, the band diagram for Topo100, calculated using 2D elasticity, is reported in Fig. 3b, with mode shapes of its edge modes at  $\xi = \pi$  shown in Fig. 2d and 2e. Both mode shapes of ML Topo90 feature in-plane and out-of-plane displacement with a high decay rate away from the top (floppy) edge, a feature expected from a polarized lattice. For comparison, mode shapes of Topo100 display similar in-plane deformation and decay rate. This observation supports the hypothesis that the flexural response of ML Topo90 will import some topological attributes from its topological layer through coupling.

To strengthen this observation, we need to quantify a link between the morphological characteristics of the ML Topo90 modes and their Topo100 in-plane counterparts. To this end, we perform a modal assurance criterion (MAC) analysis, where the quantity  $MAC = |\phi_1 \cdot \phi_2| / ((\phi_1 \cdot \phi_1)(\phi_2 \cdot \phi_2))$  estimates the degree of compatibility between two eigenvectors  $\phi_1$  and  $\phi_2$  by projecting one onto the other. The MAC values vary between 0 and 1, with 1 indicating perfect compatibility and 0 perfect orthogonality. We sweep the band diagram to find the modes of ML Topo90 that display the highest MAC correlation, at each value of  $\xi$ , to the topological modes of Topo100 (for the same  $\xi$ ). Fig. 3 highlights the spectral points on the branches of ML Topo90 whose eigenmodes are most correlated with those of either topological mode of Topo100 (blue and red markers for correlation with mode I and mode II, respectively) with color intensity proportional to the strength of correlation. It is evident that, near  $\xi = \pi$ , where the first 2 modes of ML Topo90 are spectrally isolated, the correlation with Topo100 is high, consistent with our inference from the

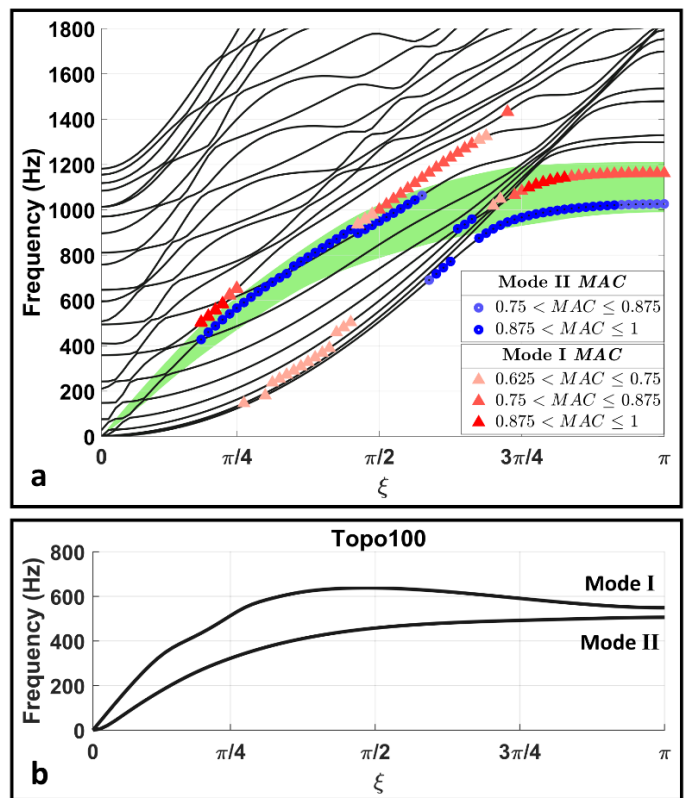


FIG. 3. (a) MAC analysis between in-plane deformation of ML Topo90 modes and Topo100 modes (shown in b); the analysis highlights the spectral points with highest modal correlation, which defines a qualitative spectral region of influence in which the bilayer response is dictated by the in-plane behavior of the topological layer.

visual inspection of the mode shapes in Fig. 2b-e. As we move away from  $\pi$ , the identified spectral points are more scattered across the available branches, as expected given the competition of several hybridizing modes at longer wavelengths. This said, the highest compatibility points remain organized along spectral paths that are qualitatively reminiscent of the Topo100 edge mode branches (Fig. 3b), and identify a spectral “region of influence” (whose qualitative support is highlighted in green in 3a) where the response of ML Topo90 is heavily controlled by the topological layer. These observations corroborate the notion that the out-of-plane response of the ML Topo90 modes is dictated by the in-plane topological behavior of the topological layer through coupling. Note that moving closer to the continuum limit increases the chance of “false positives” due to the higher morphological similarity of all modes at long wavelengths. For these reasons, we will mostly restrict our considerations to the  $\xi > \pi/2$  regime.

To illustrate the manifestation of these phenomena at the lattice scale we simulate wave propagation in an  $8 \times 19$  ML Topo90 lattice under point excitation. In order to maximize the achievable coupling and deliberately

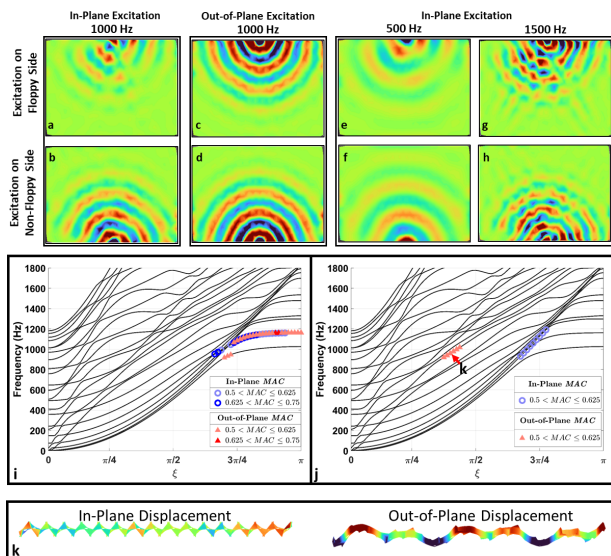


FIG. 4. Full-scale simulations. Snapshots of out-of-plane wavefields for in-plane excitation at 500, 1000, and 1500 Hz from the floppy (a,e,g) and non-floppy (b,f,h) edges; out-of-plane wavefields for out-of-plane excitation at 1000 Hz from the floppy (c) and non-floppy (d) edges; MAC analysis between response of a strip extracted from the ML Topo90 lattice wavefield (excited at 1000 Hz from the floppy (i) and non-floppy (j) edge) and ML Topo90 supercell modes available in the same spectral interval; (k) example of bulk-like mode-shape resulting from non-floppy edge excitation.

trigger the in-plane topological effects that we intend to transfer to the flexural modes, we prescribe an in-plane (force) excitation parallel to the outer face of the topological layer in the form of a 5-cycle tone burst. Fig. 4 shows snapshots of a fully developed flexural wavefield on the surface of ML Topo90 for excitation prescribed at the top/floppy and bottom/non-floppy edges, respectively, with carrier frequencies of 500 Hz (Figs. 4e and 4f), 1000 Hz (Figs. 4a and 4b), and 1500 Hz (Figs. 4g and 4h). Excitation at 1000 Hz, the interval where the topological modes fold and display the strongest polarization, reveals strong asymmetry between waves emanating from the floppy and non-floppy edges. Specifically, from the non-floppy side, waves propagate into the bulk with the isotropy and crest structure typical of flexural waves in plates, while, from the floppy side, the penetration into the bulk appears significantly more impeded and we observe some localization along the edge. It is important to note that, in this problem, we do observe waves leaking into the bulk even from the floppy edge, resulting in a weaker asymmetry between the edges than the one observed for in-plane waves by Ma et al. [27], or even than that observed in the in-plane field for this bilayer (see SM). This is due to the fact that, in the frequency interval of our burst, the band diagram of the bilayer features several flexural bulk modes than can be activated in conjunction with the topological modes. This is not the case

in a strictly in-plane problem, where the only competition to the topological edge modes at the floppy side comes from the acoustic S- and P-modes which, however, are fast and long-wavelength modes associated with modest compliance (compared to the edge modes) and negligible amplitude signatures. In contrast with the 1000 Hz case, the wavefields for excitation at 500 Hz and 1500 Hz are significantly more symmetric between the floppy and non-floppy sides. This shows that the asymmetric wave transport is frequency-selective, being mostly absorbed below and above the frequency interval of the polarized modes.

The non-triviality of this result can be appreciated by considering the complementary case where the same lattice is excited with an out-of-plane force. The scope of this test is to confirm that the effect observed is, indeed, due to topological polarization, and, as such, intrinsic to the bulk and topologically protected, and not a mere trivial consequence of any asymmetry between the local geometric features of the edges. Wavefields for an out-of-plane excitation at 1000 Hz from the floppy and non-floppy edges are shown in Fig. 4c and 4d, respectively. The response is dominated by circular-crested waves propagating into the bulk with no localization at the edges and nearly perfect symmetric behavior between the edges. If the lattice displayed any trivial edge behavior associated with the quasi-dangling elements of the edges, such effects would be magnified by this type of excitation, as the force would directly promote the out-of-plane motion of these elements. In other words, if the asymmetry were to be attributed to the slight geometric differences between the edges (that still exist despite the trimming operation discussed above), it should be even more pronounced with this excitation. This is clearly not the case here, suggesting that the asymmetry observed at 1000 Hz (Figs. 4a and 4b) must be indeed originating from the polarization of the in-plane modes.

To pinpoint which excited modes are responsible for the established asymmetry, we can again resort to MAC analysis. To this end, from Fig. 4a and b we choose a strip of 16 cells spanning the lattice from edge to edge, such that the top/bottom cell includes the excitation point, and we compare their in-plane and out-of-plane displacement fields against the eigenvectors of the ML Topo90 supercell. In Figs. 4i and 4j, the markers show the ML Topo90 modes with highest correlation with the deformation of the extracted strip at each value of  $\xi$  in the neighborhood of 1000 Hz, for excitation from the floppy (Fig. 4i) and non-floppy (Fig. 4j) edge. For excitation at the floppy edge, the two coupled topological modes are highlighted near  $\pi$  for both in-plane and out-of-plane MAC comparison. On the other hand, excitation at the non-floppy end appears to activate a different set of modes, whose eigenvectors suggest that they are predominantly bulk flexural modes lacking any topological character (Fig. 4h). This confirms that the deformation

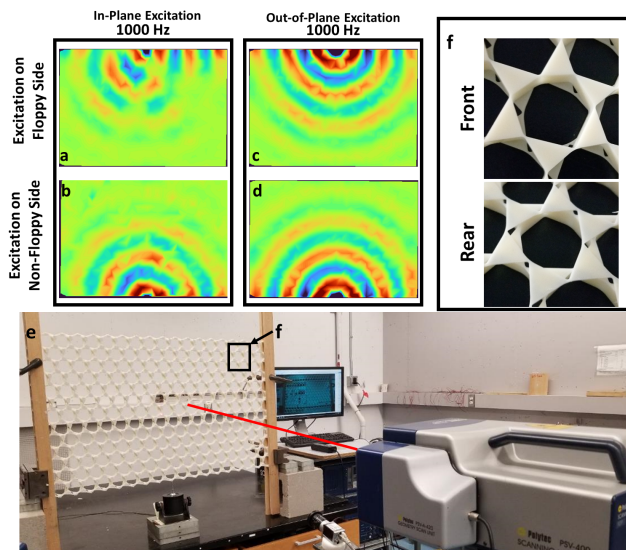


FIG. 5. Laser-assisted wave propagation experiments. Out-of-plane wavefields for in-plane excitation at 1000 Hz from the floppy (a) and non-floppy (b) edges; out-of-plane wavefields for out-of-plane excitation at 1000 Hz from the floppy (c) and non-floppy (d) edges; (e) experimental setup and (f) detail of the lattice revealing high-precision features obtained via double-side CNC machining.

observed in Fig. 4a are, indeed, rooted in the topological in-plane modes.

To verify these phenomena experimentally, we perform laser-assisted (Polytec PSV 400 3D Laser Doppler Vibrometer) experiments on a  $7 \times 17$ -cell ML Topo90 lattice prototype manufactured via double-side computer numerical control (CNC) precision machining from a sheet of ABS (see SM for details). The excitation burst is applied by a shaker with the stinger placed parallel to the lattice plane and probing the outer face of the topological layer. The laser scans the lattice surface, measuring the out-of-plane velocity at one point per triangle. The experimental setup is shown in Fig. 5e, with detailed close-ups of the specimen in Fig. 5f. Representative wavefield snapshots for a 1000 Hz in-plane excitation at the floppy and non-floppy side are shown in Fig. 5a and 5b, respectively, while snapshots for an out-of-plane excitation at the floppy and non-floppy edge are shown in Fig. 5c and 5d, respectively. The results match the simulations nicely. The in-plane excitation triggers an asymmetric response from the floppy/non-floppy edge, with localization at the floppy side, and isotropic propagation into the bulk from the non-floppy side; in contrast, the out-of-plane excitation triggers flexural bulk waves and is virtually insensitive to lattice polarization. For completeness, we also performed experiments for in-plane and out-of-plane excitations at 500 Hz and 1500 Hz. We report that, for in-plane excitation, some asymmetry persists at these frequencies, particularly at 500 Hz. The reasons behind this discrepancy with the computational model likely lie

in the experimental complexity and limitations of our spectral processing tools. More work will be required to provide an exhaustive explanation for this behavior, but some initial conjectures addressing this point are provided in the SM.

In conclusion, by designing a bilayer with in-plane to out-of-plane coupling capabilities we have demonstrated the ability to export topological modes from their native in-plane elastodynamics to the flexural realm. These results open the doors to the application of topological wave manipulation strategies to thin structures traditionally designed to operate in bending.

This work is supported by the National Science Foundation (NSF Grant No. EFRI-1741618). We acknowledge the help of Peter Ness at the UMN CSE shop for his expert assistance with the specimen fabrication.

- 
- [1] J. C. Maxwell, L. on the calculation of the equilibrium and stiffness of frames, *The London, Edinburgh, and Dublin Philosophical Magazine and Journal of Science* **27**, 294 (1864).
  - [2] T. C. Lubensky, C. L. Kane, X. Mao, A. Souslov, and K. Sun, Phonons and elasticity in critically coordinated lattices, *Reports on Progress in Physics* **78**, 073901 (2015).
  - [3] X. Mao and T. C. Lubensky, Coherent potential approximation of random nearly isotropic kagome lattice, *Phys. Rev. E* **83**, 011111 (2011).
  - [4] X. Mao and T. C. Lubensky, Maxwell lattices and topological mechanics, *Annual Review of Condensed Matter Physics* **9**, 413 (2018), <https://doi.org/10.1146/annurev-conmatphys-033117-054235>.
  - [5] A. Souslov, A. J. Liu, and T. C. Lubensky, Elasticity and response in nearly isotropic periodic lattices, *Phys. Rev. Lett.* **103**, 205503 (2009).
  - [6] N. A. Fleck and X. Qiu, The damage tolerance of elastic-brittle, two-dimensional isotropic lattices, *Journal of the Mechanics and Physics of Solids* **55**, 562 (2007).
  - [7] H. Fan, F. Meng, and W. Yang, Sandwich panels with kagome lattice cores reinforced by carbon fibers, *Composite Structures* **81**, 533 (2007).
  - [8] D. D. Symons and N. A. Fleck, The Imperfection Sensitivity of Isotropic Two-Dimensional Elastic Lattices, *Journal of Applied Mechanics* **75**, 10.1115/1.2913044 (2008), 051011, [https://asmigitalcollection.asme.org/appliedmechanics/article-pdf/75/5/051011/5477570/051011\\_1.pdf](https://asmigitalcollection.asme.org/appliedmechanics/article-pdf/75/5/051011/5477570/051011_1.pdf).
  - [9] Y. Zhang, X. Qiu, and D. Fang, Mechanical properties of two novel planar lattice structures, *International Journal of Solids and Structures* **45**, 3751 (2008), special Issue Honoring K.C. Hwang.
  - [10] A. S. Phani, J. Woodhouse, and N. A. Fleck, Wave propagation in two-dimensional periodic lattices, *The Journal of the Acoustical Society of America* **119**, 1995 (2006), <https://doi.org/10.1121/1.2179748>.
  - [11] M. Schaeffer and M. Ruzzene, Wave propagation in reconfigurable magneto-elastic kagome lattice structures, *Journal of Applied Physics* **117**, 194903 (2015),

- <https://doi.org/10.1063/1.4921358>.
- [12] E. Riva, D. E. Quadrelli, G. Cazzulani, and F. Braghin, Tunable in-plane topologically protected edge waves in continuum kagome lattices, *Journal of Applied Physics* **124**, 164903 (2018), <https://doi.org/10.1063/1.5045837>.
- [13] H. Chen, H. Nassar, A. N. Norris, G. K. Hu, and G. L. Huang, Elastic quantum spin hall effect in kagome lattices, *Phys. Rev. B* **98**, 094302 (2018).
- [14] S. Gonella, Symmetry of the phononic landscape of twisted kagome lattices across the duality boundary, *Physical Review B* **102**, 140301 (2020).
- [15] V. Kapko, M. M. Treacy, M. F. Thorpe, and S. Guest, On the collapse of locally isostatic networks, *Proceedings of the Royal Society A: mathematical, physical and engineering sciences* **465**, 3517 (2009).
- [16] Z. Gao, D. Liu, and D. Tománek, Two-dimensional mechanical metamaterials with unusual poisson ratio behavior, *Physical Review Applied* **10**, 064039 (2018).
- [17] K. Sun, A. Souslov, X. Mao, and T. C. Lubensky, Surface phonons, elastic response, and conformal invariance in twisted kagome lattices, *Proceedings of the National Academy of Sciences* **109**, 12369 (2012), <https://www.pnas.org/content/109/31/12369.full.pdf>.
- [18] J. Ma, J.-W. Rhim, L. Tang, S. Xia, H. Wang, X. Zheng, S. Xia, D. Song, Y. Hu, Y. Li, B.-J. Yang, D. Leykam, and Z. Chen, Direct observation of flatband loop states arising from nontrivial real-space topology, *Phys. Rev. Lett.* **124**, 183901 (2020).
- [19] R. Süsstrunk and S. D. Huber, Observation of phononic helical edge states in a mechanical topological insulator, *Science* **349**, 47 (2015).
- [20] X.-L. Qi and S.-C. Zhang, Topological insulators and superconductors, *Rev. Mod. Phys.* **83**, 1057 (2011).
- [21] M. Z. Hasan and C. L. Kane, Colloquium: Topological insulators, *Rev. Mod. Phys.* **82**, 3045 (2010).
- [22] J. Ma, K. Sun, and S. Gonella, Valley hall in-plane edge states as building blocks for elastodynamic logic circuits, *Physical Review Applied* **12**, 044015 (2019).
- [23] D. Z. Rocklin, B. G.-g. Chen, M. Falk, V. Vitelli, and T. C. Lubensky, Mechanical weyl modes in topological maxwell lattices, *Phys. Rev. Lett.* **116**, 135503 (2016).
- [24] C. Kane and T. Lubensky, Topological boundary modes in isostatic lattices, *Nature Physics* **10**, 39 (2014).
- [25] H. Kedia, A. Souslov, and D. Z. Rocklin, Soft topological modes protected by symmetry in rigid mechanical metamaterials, *Phys. Rev. B* **103**, L060104 (2021).
- [26] D. Z. Rocklin, S. Zhou, K. Sun, and X. Mao, Transformable topological mechanical metamaterials, *Nature communications* **8**, 1 (2017).
- [27] J. Ma, D. Zhou, K. Sun, X. Mao, and S. Gonella, Edge modes and asymmetric wave transport in topological lattices: Experimental characterization at finite frequencies, *Physical review letters* **121**, 094301 (2018).
- [28] O. Stenull and T. C. Lubensky, Signatures of topological phonons in superisostatic lattices, *Phys. Rev. Lett.* **122**, 248002 (2019).
- [29] G. Baardink, A. Souslov, J. Paulose, and V. Vitelli, Localizing softness and stress along loops in 3d topological metamaterials, *Proceedings of the National Academy of Sciences* **115**, 489 (2018), <https://www.pnas.org/content/115/3/489.full.pdf>.
- [30] O. Stenull, C. L. Kane, and T. C. Lubensky, Topological phonons and weyl lines in three dimensions, *Phys. Rev. Lett.* **117**, 068001 (2016).
- [31] O. R. Bilal, R. Süsstrunk, C. Daraio, and S. D. Huber, Intrinsically polar elastic metamaterials, *Advanced Materials* **29**, 1700540 (2017).
- [32] P. Celli, S. Gonella, V. Tajeddini, A. Muliana, S. Ahmed, and Z. Ounaies, Wave control through soft microstructural curling: bandgap shifting, reconfigurable anisotropy and switchable chirality, *Smart Materials and Structures* **26**, 035001 (2017).
- [33] V. Giurgiutiu, Tuned lamb wave excitation and detection with piezoelectric wafer active sensors for structural health monitoring, *Journal of Intelligent Material Systems and Structures* **16**, 291 (2005), <https://doi.org/10.1177/1045389X05050106>.

# Supplemental Materials: Topological Flexural Modes in Polarized Bilayer Lattices

Mohammad Charara,<sup>1</sup> Kai Sun,<sup>2</sup> Xiaoming Mao,<sup>2</sup> and Stefano Gonella<sup>1,\*</sup>

<sup>1</sup>*Department of Civil, Environmental, and Geo- Engineering,  
University of Minnesota, Minneapolis, MN 55455, USA*

<sup>2</sup>*Department of Physics, University of Michigan, Ann Arbor, Michigan 48109, USA*

## Dangling Trivial Edge Modes in a Bi-layer Topological Lattice prior to Edge Clipping

We deliberately amend the lattice edges by trimming, as much as possible, the protruding portion of the edge cells, which could behave as quasi-dangling elements. With this correction, we aim to minimize any trivial edge effects associated with these elements that may manifest in the form of flexural mechanisms localized in the protruding portion of either edge. Such mechanisms, if established, would be trivial in that they cannot be linked to any topological polarization and strictly depend on the specific geometric features of the edges. While trivial edge effects are modest in in-plane problems, their flexural counterparts can display large amplitudes, with the possibility to pollute, if not overshadow, the actual topological effects that we seek to observe. This correction virtually eradicates this possibility, thus distilling the topological contribution from the polarized layer. In performing this correction, we exploit the notion of topological protection, whereby perturbations of the edge geometry do not affect the polarization, which is solely a property of the bulk.

To demonstrate how the establishment of strong trivial behavior would be disruptive for our analysis, in Fig. S1a we show the band diagram of the lattice prior to edge clipping, with the lattice shown in the inset and the supercell highlighted and shown next to it. In-plane displacement (with color proportional to displacement in the  $y$  direction) and out-of-plane displacement (with color proportional to out-of-plane displacement) for modes 1, 2, and 5 at  $\xi = \pi$  are shown in Fig. S1b, c, and d, respectively. While the behavior of mode 1 is qualitatively analogous to that discussed for the trimmed edge, the interpretation of mode 2 becomes more problematic. Here we see a very aggressive localization of out-of-plane displacement on the left (floppy) edge. Although a localization at this edge is nominally what we want, it is clear that the localization here is concentrated in the last half cell and can be attributed to the quasi-dangling nature of the protruding element, rather than polarization in the bulk. Perhaps more importantly, if we inspect mode 5 (a mode we don't discuss in the paper because of its lack of interesting features in the edge-clipped version of this structure) we

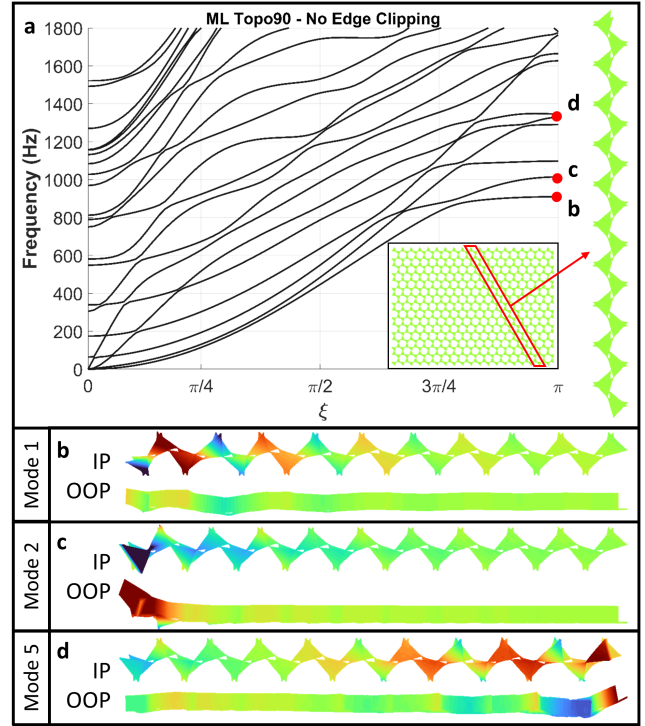


FIG. S1. (a) ML Topo90 band diagram prior to edge clipping, with lattice in the bottom right corner inset and supercell highlighted; in-plane and out-of-plane displacement for modes 1 (b), 2 (c), and 5 (d) of ML Topo90 prior to edge clipping.

see that it displays a similar aggressive out-of-plane localization on the right (non-floppy edge), acting as the trivial twin of mode 2. In addition, its out-of-plane localization is incommensurate to its in-plane displacement pattern, which is not very localized, featuring a long decay rate that reaches the floppy edge of the supercell, confirming that this purely flexural behavior is simply due to the quasi-dangling nature of the edge triangle, and not triggered by topological in-plane modes. When wave-propagation experiments are attempted with this lattice, two things make topological behavior observations very difficult: mode 2 highly controls the displacement at the floppy edge (drowning out the seemingly topological mode 1 due to spectral proximity), and mode 5 displays similar localization on the non-floppy edge (obscuring the asymmetric wave transport properties of the bulk). When we clip the edges of the lattice, mode 2 and mode 5 experience a vast morphological change, and

\* sgonella@umn.edu

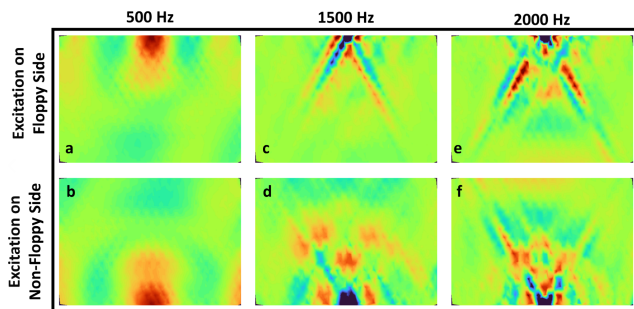


FIG. S2. Simulated in-plane displacement wavefields for in-plane excitation from the floppy and non-floppy side at frequencies of 500 Hz (a and b), 1000 Hz (c and d), and 1500 Hz (e and f), respectively.

mode 1 and 2 become highly topologically influenced.

### Simulations - In-Plane Displacement Wavefields

In-plane displacement wavefields for the computational wave propagation simulations help enrich our understanding of the wave transport characteristics of this bi-layer lattice. Fig. S2 shows in-plane displacement wavefields (in the  $y$  direction) for excitation at the floppy and non-floppy edges at carrier frequencies of 500 Hz (S2a and b), 1000 Hz (S2c and d), and 1500 Hz (S2e and f). The in-plane response shows frequency selectivity and asymmetry. At 1000 Hz, the wavefield is highly asymmetric when excited from the floppy and non-floppy end; we see high impedance into the bulk in the floppy edge excitation case. Notably, from both edges, we recognize an in-plane footprint similar to that of reference [1]: the non-floppy edge shows almost perfect isotropic wave propagation, while the floppy-edge features some directionality. Note that excitation from the floppy end does display some leakage into the bulk, likely due to the influence of the twisted kagome layer, which is non-polarized; however this effect is almost insignificant compared to the isotropic wave propagation seen from the non-floppy end. These results come to no surprise given that topological behavior is native to in-plane mechanics and thus we expect to observe its signature in the in-plane wavefields.

### Lattice Manufacturing

The bi-layer lattice was manufactured via CNC machining; an image of the manufacturing process is shown in S3. Due to the complexity of this structure, the machining was done in two steps. First, a plastic plate was fastened to a previously machined manufacturing plate and the twisted kagome layer was milled to 10% of the total thickness. The structure was then flipped over to the opposing face, reattached to the manufacturing plate,

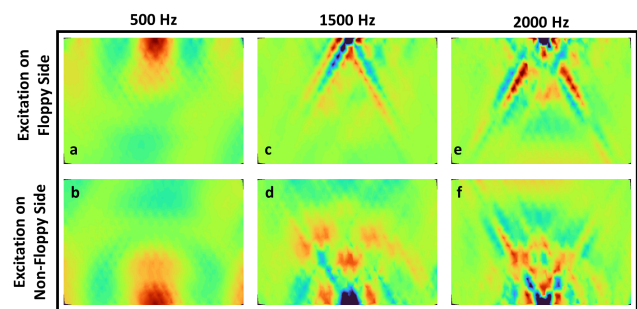


FIG. S3. Manufacturing of the bi-layer lattice via double-sided CNC machining (cutting of the topological layer shown).

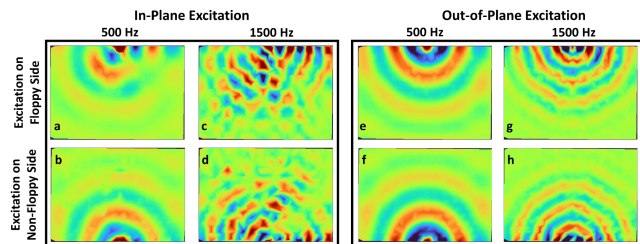


FIG. S4. Laser-assisted wave propagation experiments - out-of-plane wavefield snapshots due to in-plane excitation from the floppy and non-floppy edges at 500 Hz (a and b) and 1500 Hz (c and d); out-of-plane wavefield snapshots due to out-of-plane excitation from the floppy and non-floppy edges at 500 Hz (e and f) and 1500 Hz (g and h).

and the topological kagome layer was milled. The result is a bi-layer lattice made from one single piece of ABS plastic.

### Supplemental Experimental Wavefields

Fig. S4 shows wavefield snapshots for in-plane excitations from the floppy and non-floppy edges at carrier frequencies of 500 Hz (Fig. S4a and b) and 1500 Hz (Fig. S4c and d), and for out-of-plane excitation from the floppy and non-floppy edges at 500 Hz (Fig. S4e and f) and 1500 Hz (Fig. S4g and h). Out-of-plane excitation results show that, indeed, this effect is not trivial and that this type of excitation only induces waves propagating isotropically regardless of excited edge, an expected result because in-plane mechanics are a required mediator to trigger the desired topological behavior. However, somewhat surprisingly, we found that the asymmetric behavior experienced by the lattice for in-plane excitation of 1000 Hz persists at 500 Hz and 1500 Hz, albeit in a much weaker form, especially for the latter. This may be due to a number of imperfections, which are difficult to control in an experimental setting, that may deviate from its nominal numerical counterpart. Specifically, there may exist a slight spectral mismatch between the lattice used in simulations and the actual prototype due

to some meshing shortcomings (i.e. in mesh size or structure) in our computational model which we could curb, but not fully remove, within the limitations of our computational platform. Another factor could be the much lower number of visualization points used in the experiment (two displacement scanning locations per unit cell) vs the simulation (about 1100 nodes per unit cell). These discrepancies require more investigations and will be further studied in our future work.

- 
- [1] J. Ma, D. Zhou, K. Sun, X. Mao, and S. Gonella, Edge modes and asymmetric wave transport in topological lattices: Experimental characterization at finite frequencies, *Physical review letters* **121**, 094301 (2018).